Efficient nanoparticles removal and bactericidal action of electrospun nanofibers membranes for air filtration

Ana Claudia Canalli Bortolassi, Sakthivel Nagarajan, Bruno de Araújo Lima, Vádila Giovana Guerra, Mônica Lopes Aguiar, Vincent Huon, Laurence Soussan, David Cornu, Philippe Miele, Mikhael Bechelany

EFFICIENT NANOPARTICLES REMOVAL AND BACTERICIDAL ACTION OF ELECTROSPUN NANOFIBERS MEMBRANES FOR AIR FILTRATION

Ana Claudia Canalli Bortolassi[1], Sakthivel Nagarajan[2], Bruno de Araújo Lima[1], Vádila Giovana Guerra[1], Mônica Lopes Aguiar[1], Vincent Huon[3], Laurence Soussan[2], David Cornu[2], Philippe Miele[2] and Mikhael Bechelany[2]

[1]Universidade Federal de São Carlos – UFSCar, Departamento de Engenharia Química, Rodovia Washington Luiz, km 235 – SP 310, 13565-905 São Carlos, Brazil; tel. +55 16 3351 8269

[2]Institut Européen des Membranes, IEM – UMR 5635, ENSCM, CNRS, Univ Montpellier, Montpellier, France

[3]Laboratoire de Mécanique et Génie Civil, Université de Montpellier, CNRS, 34090, Montpellier, France

E-mail: mikhael.bechelany@umontpellier.fr

ABSTRACT

Human exposure to air pollution and especially to nanoparticles is increasing due to the combustion of carbon-based energy vectors. Fibrous filters are among the various types of equipment potentially able to remove particles from the air. Nanofibers are highly effective in this area; however, their utilization is still a challenge due to the lack of studies taking into account both nanoparticle collection efficiency and antibacterial effect. The aim of this work is to produce and evaluate novel silver/polyacrylonitrile (Ag/PAN) electrospun fibers deposited on a nonwoven substrate to be used as air filters to remove nanoparticles from the air and also showing antibacterial activity. In order to determine the optimum manufacturing conditions, the effects of several electrospinning process parameters were analyzed such as solution concentration, collector to needle distance, flow rate, voltage, and duration. Ag/PAN nanofibers were characterized by X-ray diffraction (XRD), Transmission Electron Microscopy (TEM), Fourier Transform Infra-Red spectroscopy (FTIR), Energy-dispersive X-ray spectroscopy (EDX), X-ray photoelectron spectroscopy (XPS), and Scanning Electron Microscopy (SEM). In addition, filtration performances were determined by measuring the pressure drop and collection efficiency of sodium chloride (NaCl) aerosol particles (9 to 300 nm diameters) using Scanning Mobility Particle Sizers (SMPS). Filters with high filtration efficiency (≈100%) and high-quality factor (≈0.05 Pa^{-1}) were obtained even adding different concentrations of Ag nanoparticles (AgNPs) to PAN nanofibers. The resultant Ag/PAN nanofibers showed excellent antibacterial activity against 10^4 CFU/ml *E.coli* bacteria.

Keywords: air filtration, bactericidal material, electrospinning, nanofibers, silver

Introduction

Researches related to filter materials with high filtration efficiency and antibacterial activity have received great interest in recent years due to the currently impressive levels of environmental particular matter (PM) pollution and the diseases caused by these particles [1-3]. It has been reported that bacteria account for more than 80% of the inhalable microorganisms in PM, which are responsible for the transmission of respiratory diseases and allergies [4], making air filters with bactericidal properties highly desired.

Membrane filtration is nowadays considered to be the most efficient and reliable physical method for protection from air pollutants [5] but filters with low-pressure drop, high-quality factor, and antibacterial properties are still a challenge to be produced. According to Vinh and Kim [6], filters must be designed to be durable and effective, while maintaining a low-pressure drop, to display a long lifetime, to be easy to handle, to have low production cost and a small package space, and to be flexible for each specific demand. The control over air/waterborne pollutants, hazardous biological agents, as well as allergens, are the main requirements of food, pharmaceuticals and biotechnology industries [7]. Cleanrooms technology could be understood as activities to control and reduce product contamination and often use nanofibers filters to remove unwanted particles from the air. Semiconductor industry has already highlighted the use of this technology, however, automotive and space industry are still discovering the advantages of a certain level of cleanliness over the quality and reliability of the final product [8].

Different types of fiber filters as conventional, glass fibers, melt-blown and spunbond fibers have been widely used in different air filtration applications but show relatively low filtration efficiency with respect to fine particles due to the materials' microsized fiber diameter and large pore size [9]. Electrospun nanofibrous membranes are among attractive air filters that exhibit fascinating features, including higher molecular orientation fibers and larger tensile strength than films. Recent study demonstrated that electrospun nanofibers showed excellent mechanical properties [10] and thermal stability [11]. Other special properties, such as large specific surface area, high porosity, small pore size, and good interconnected pore structure, which is conducive to the capture of fine particles [10-13], provide electrospun polymer nanofibers applications in the filtration and textile fields [16]. Nanofiber membranes demonstrate superior filtration performances compared to the traditional filtration materials [17] by measuring the penetration of sodium chloride (NaCl) nanoparticles [18], [19].

Electrospinning is among the numerous methods currently available to produce nanofibers which continues to motivate the development of novel nanotechnology due to their extraordinary properties including small fiber diameters and the concomitant large specific surface areas, as well as the capabilities to control pore size among nanofibers and to incorporate antimicrobial agents at nanoscale [17-19]. Nevertheless, this is still a challenge to produce appropriate nanofibers for separation and filtration applications [22], such as protective masks to capture PM2.5 [23]. Solution concentration, flow rate, collector to needle distance, voltage and duration are analyzed in order to achieve optimum manufacturing conditions of electrospinning. Changing the polymer concentration can vary the solution viscosity and higher

viscosity favors formation of fibers without polymer beads. The surface tension is driven toward the formation of the beads and thus, the reduced surface tension will increase the formation of the fibers without beads [24]. Small fiber diameter leads to better filtration efficiency. This explains the dramatically decrease from 98% to 48% of removal efficiencies of PAN air filters when the fiber diameter increased from 200 nm to 1 µm, such as shown by Liu *et al*.[2].

Many types of electrospun fibrous membranes (Nylon 6, polyethylene oxide, alumina nanofibers) have been fabricated for air filtration [25]–[27]. Polyacrylonitrile (PAN) is among the various polymeric materials which is widely used for filtration due to easy fiber formation by electrospinning with unique thermal stability, high mechanical properties and good solvent resistance [26–29]. Usually, nanofibrous membranes have high filtration efficiency for fine particles but also an excessive pressure drop [9]. Choosing a suitable mat to deposit nanofibers is also necessary to achieve resistant and permeable fibrous filter.

It is very important to display antimicrobial properties on the fibrous filter medium, especially when they are used as respiratory protection and for indoor air purification [32]. Silver (Ag) is particularly attractive among metal nanoparticles because of its significant widespread use in biology, antimicrobial properties, optical properties, and oxidative catalysis applications. It is also widely used and recognized as a broad-spectrum biocidal agent which is non-toxic to human cells and effective against bacteria, fungi, and viruses [31–34]. The antimicrobial activity of silver nanoparticles might be originated from their capability to attach to the surface of cell membranes, thus disturbing permeability and respiration functions of the microbes [37]. The combination of the high specific surface area and fineness of electrospun nanofibers with the biocidal activity of Ag nanoparticles results in a superior and versatile antimicrobial material [38]–[40].

However, nanofibers produced by adding Ag nanoparticles directly into the electrospinning polymer solutions have demonstrated decreased in antimicrobial efficiency due to AgNPs aggregation and subsequently reduced bioavailability [41]. Lala *et al*. [42] studied different polymers and concluded that PAN acts as a stabilizing agent to inhibit the agglomeration of silver nanoparticles. DMF is used as a solvent and it is also able to reduce Ag ions to the metallic silver even at room temperature and without using any reducing agent [28], [43], [44]. Although there are some studies related to Ag/polymer electrospun nanofibers used on catalytic degradation [45], their application in air filtration is still poorly explored [46],[47].

In this paper, we explore the design of uniform Ag/PAN nanofibers with not only bactericidal activity but also with excellent air filtration performance. Silver/polyacrylonitrile (Ag/PAN) fibers were deposited on the nonwoven substrate by electrospinning. In order to determine the optimum manufacturing conditions, the effects of several electrospinning process parameters were analyzed such as solution concentration, collector to needle distance, flow rate, voltage, and duration. Ag/PAN nanofibers were characterized by X-ray diffraction (XDR), Transmission Electron Microscopy (TEM), Fourier Transform Infra-Red spectroscopy (FTIR), Energy-dispersive X-ray spectroscopy (EDX), X-ray photoelectron spectroscopy (XPS) and Scanning Electron Microscopy (SEM). Viscosity, conductivity, thickness, porosity,

permeability and pressure drop were also determined. In addition, filtration performances were determined by measuring the penetration of sodium chloride (NaCl) aerosol particles (9 to 300 nm diameters) using Scanning Mobility Particle Sizers (SMPS). The antibacterial activity against *E.coli* bacteria of the resultant Ag/PAN nanofibers was also investigated.

Experimental

Materials

Polyacrylonitrile (PAN; M_w~150,000 g/mol; CAS Number 25014-41-9), N,N-Dimethylformamide (DMF; 99.8%; CAS number 68-12-2) and silver nitrate ($AgNO_3$; M_w~ 169.87 g/mol; CAS number 7761-88-8) were purchased from Sigma Aldrich. The substrate to collect nanofibers was obtained from Freudenberg and was made by Polyethylene terephthalate (PET) fibers. Sodium chloride (NaCl; 99%; CAS number 7647-14-5) was used to generate nanoparticles to evaluate the removal efficiency and was purchased from Sigma Aldrich.

Methods

Preparation of Ag/PAN nanofibers

Nanofibers were prepared using 9.1 % (w/v) PAN polymer solution. The PAN polymer solution was prepared using dimethylformamide (DMF) as a solvent. After 2 hours of agitation, different percentages of $AgNO_3$ (0, 1, 10, 50 wt%; w.r.t polymer) were added. Solutions were kept stirring for 48 h protected from light at room temperature to form a homogenous solution. It was possible to notice the color change from colorless to yellow-brown indicating the Ag nanoparticles formation [42], [48].

Viscosity and conductivity of the solution was analyzed to comprehend how the addition of AgNPS changed the nanofibers characteristics. Viscosity was measured using a Brookfield viscometer spindle 29 (TC-650, AMETEK Brookfield) and conductivity by an electrical conductivity meter (TEC-4MP, Tecnal).

PAN solution containing Ag nanoparticles was loaded in a 12 ml syringe with an attached 0.7 mm diameter needle. A syringe pump (KDS 100, KDScientific) was used to feed the solution in the electrospinning lab-made system [49]. The flow rate of the solution was fixed to 0.2 ml/h and 25 kV power was supplied using a High Voltage Power Supply (T1CP 300 304n-iSeg). PET films wrapped around the rotating machine were used to collect the fibers. The distance between the syringe tip and the collector was kept at 15 cm. Filter media prepared were denoted as 0AgF, 1AgF, 10AgF and 50AgF using 0wt% $AgNO_3$, 1wt% $AgNO_3$, 10wt% $AgNO_3$ and 50wt% $AgNO_3$, respectively.

Structural and morphological properties of nanofiber filters

Fourier transform infrared (FTIR) spectra were recorded on a Nicolet 370 FTIR spectrometer using an ATR system. Energy-dispersive X-ray spectroscopy analysis (EDX) and elemental mapping were taken with a Zeiss EVO HD15 microscope coupled with an Oxford X-MaxN EDX detector to measure the atomic

percentage. XPS analysis was performed using a Thermoelectron ESCALAB 250 device. The X-ray excitation was provided by a monochromatic Al-Kα (hυ=1486.6 eV) source. Scanning electron microscopy (SEM) images were used to understand the morphology of the electrospun fibers using Hitachi S4800, Japan. The samples were platinum sputter-coated before observing the morphology. Electrospun fibers were deposited on the transmission electron microscopy (TEM) copper grid which is mounted on the fiber collector plate. Fibers deposited on the copper grid was observed using TEM (JEOL 2200 FS) to understand the silver nanoparticle distribution. Concentration of silver in electrospun fibers were quantified using atomic absorption spectrometer (AAnalyst 400, PerkinElmer). Accurately weighed electrospun fibers were sintered at 600°C for 6 hours and dissolved using concentrated Nitric acid. Furthermore, dissolved solution were diluted into 100 mL and employed for measuring silver concentration using AAS. samples were tensile strength of the electrospun fibers was tested using MTS 1/ME instrument, 500N load cell with the crosshead speed of 3 mm/min. Young's modulus were calculated from the linear elastic region of the stress-strain curve. Displacement data were obtained from digital image correlation analysis. Results were averaged from n=7 analysis and the student T test statistical analysis was performed to determine the significant difference between the samples. Thickness was measured using a caliper rule (Starrett) and filters were weighted to compare the mass deposition. Porosity was determined theoretically in order to evaluate the void fraction between the fibers using Ergun (1952) Equation (Eq.01):

$$\frac{\Delta P}{L} = \frac{150(1-\varepsilon)^2 \mu v_s}{\varepsilon^3 d_p^2} + \frac{1.75(1-\varepsilon)\rho_g v_s^2}{\varepsilon^3 d_p} \quad (01)$$

where (ρ_g) is the relating gas density, (μ) is the gas viscosity, (ε) is the porosity, (v_s) is the filtration superficial velocity, (d_p) is the particle diameter and (L) is the thickness of the filter media.

Filter media permeability experiments were performed varying the flow rate from 100 to 1000 mL/min and the pressure drop was measured using a digital manometer (VelociCalc Model 3A-181WP09, TSI) connected to filtration apparatus as shown in Figure 1, and as described in reference [51]. Permeability constant (k_1) was evaluated using the following equation:

$$\frac{\Delta P}{L} = \frac{\mu}{k_1} v_s \quad (02)$$

Filtration performance of nanofiber filters

Comparison between the experimental and theory collection efficiency of filter media is made using the following equation [52]:

$$n_t = n_d + n_i + n_{id} + n_g + n_e \quad (03)$$

where the total collection efficiency (n_t) is the sum of diffusion (n_d), inertial (n_i), interception (n_{id}), gravitational (n_g) and electrophoretic (n_e) mechanisms. Hinds [52] explains better each individual mechanism and the resulting curves of various filtration mechanisms. In his study, it is possible to notice that

diffusion is more active for particles smaller than 0.2 μm whereas inertial and interception for particles bigger than 1 μm. Diffusion, inertial and interception are the most important mechanisms in this work and they depend on several parameters as air velocity, fiber and particle diameter, porosity and others.

Figure 1 represent the experimental unit used in this work which consists of an air compressor (Shultz), air purification filters (Model A917A-8104N-000 and 0A0-000), atomizer aerosol generator (Model 3079, TSI), diffusion dryer (Norgren), Kriptônio and Americium neutralizing source (Model 3054, TSI), filter apparatus, flow meter size 3 (Gilmont) and SMPS device formed by electrostatic classifier (Model 3080, TSI), differential mobility analyzer and ultrafine particles counter (Model 3776, TSI).

Filtration tests were performed maintaining the surface speed (5 cm/s), the flow rate (1500 ml/min) and the filtration area (5.3 cm^2) constant. It was possible to obtain the particle diameters distribution at the beginning of filtration from 5 g/L of NaCl solution. After one hour of filtration, upstream and downstream particle distributions were measured to obtain the efficiency of the filter media using particle analyzer by electric mobility. This process has been repeated three times in order to have an average efficiency and a standard deviation.

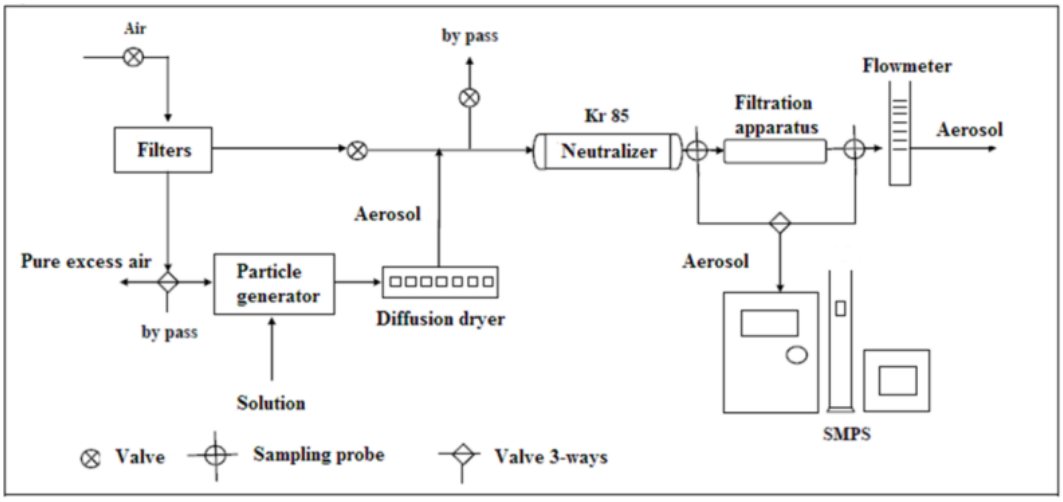

Figure 1 – Schematic of permeability and nanoparticle removal efficiency equipment [53]

Quality factor (Q_F) is another representative analyze which measure the performance of the filter media and it was evaluated relating pressure drop to removal efficiency of 100 nm diameter particles as defined by the equation below:

$$Q_F = \frac{-\ln(1-\eta)}{\Delta P} \tag{04}$$

where pressure drop across the filter is represented by ΔP and removal efficiency by η.

Bactericidal activity

Antibacterial tests were done with non-pathogenic Gram-negative *Escherichia coli* bacteria (K12 DSM 423, from DSMZ, Germany). Lysogeny broth (LB) Miller culture medium was used for bacteria cultivation, counting, and agar diffusion tests. For each experiment, a new bacterial suspension was prepared from frozen aliquots of *E. coli* stored at -20°C. Firstly, the aliquots were rehydrated in LB medium for 3 hours at 30°C and 160 rpm stirring. Then, rehydrated aliquots were inoculated into fresh LB medium (5 % v/v) and incubated overnight at 30°C under constant stirring (160 rpm) to reach the stationary growth phase. After that, the cultivated bacterial suspensions were collected by centrifugation (10 min at 4000 rpm) and the culture medium was discarded to remove nutrients from the LB medium. The recovered pellets were suspended in spring water (Cristaline Sainte Cécile, France: $[Ca^{2+}]$ = 39 mg/L, $[Mg^{2+}]$ = 25 mg/L, $[Na^{+}]$ = 19 mg/L, $[K^{+}]$ = 1.5 mg/L, $[F^{-}]$ < 0.3 mg/L, $[HCO_3^{-}]$ = 290 mg/L, $[SO_4^{2-}]$ = 5 mg/L, $[Cl^{-}]$ = 4 mg/L, $[NO_3^{-}]$ < 2 mg/L) to avoid further bacterial growth. The absorbance of the bacterial suspension was measured at 600 nm to assess the bacterial concentration according to a calibration curve obtained previously at the Laboratory. The bacterial cells were finally diluted in spring water to obtain bacterial concentrations ranging from 10^8 to 10^3 CFU/mL. In order to assess the biocide action of the Ag/PAN material surface, contact tests were first carried out on agar plates. A small volume (40 µL) of a bacterial suspension at about 10^3 CFU/mL was deposited respectively on sterile PAN and on Ag/PAN (with Ag 1wt%); the material pieces having the same size (2.25 cm^2). The materials were then put in contact with a nutritive LB agar for 6 h and removed. The plates were incubated overnight at 37°C to allow the bacterial colonies to grow and the colonies were thereafter counted, knowing that each colony stemmed from one initial bacterium. A blank was simultaneously done and consisted in depositing the bacterial suspension directly on the LB agar. Each test was triplicated.

Liquid tests were also performed to complete the antibacterial characterization of the nanofibers. Reactors used for the liquid bactericidal tests were 10 mL-glass tubes equipped with a breathable cap. For each test, reactors were filled with 10 mL of the bacterial suspension and a piece of Ag/PAN material (2.25 cm^2) was immersed inside the bacterial suspension. Reactors were then incubated for 5 hours, at room temperature (20 ± 2°C) and under constant stirring (160 rpm), protected from light by an aluminum foil. Control reactors were carried out simultaneously: (i) with bacteria solely (i.e. without material) and (ii) with a piece of PAN (2.25 cm^2) that was prior disinfected by UVC irradiation for 30 min. The bacterial concentrations were monitored in the reactor by plaque assay method and their growth was correlated to the bactericidal performances of the material.

For the plaque assay method, each sample was immediately diluted in 0.9% saline solution (NaCl) to neutralize the effect of any Ag(+) that might have been released from the material. Each dilution was spread onto specific nutrient agar and incubated overnight at 37°C. Once the bacteria had grown on plates, the colonies were counted. All experiments were performed twice and the concentrations of bacteria in the sample were calculated as the average of the number of colonies divided by the volumes inoculated on the specific agar, with the corresponding dilution factor taken into account. The quantification limit was

25 CFU/mL. At the end of each liquid bactericidal kinetics (i.e. after 5 h), a quantitative analysis of the silver desorbed from the material was performed. For these analyses, each sample was diluted two times with 0.2% HNO_3 to completely solubilize the silver. Prior to solubilization, samples could be filtrated on Millipore 0.2 µm cellulose acetate filters to retain any large silver nanoparticles that could have been released from the material. Then, the samples were analyzed by Atomic Absorption Spectrometry (AAnalyst 400, PerkinElmer).

Results and discussion

PAN nanofiber filters containing different amounts of Ag nanoparticles were synthesized by electrospinning. Produced filter media were denoted as 0AgF, 1AgF, 10AgF and 50AgF using 0wt% $AgNO_3$, 1wt% $AgNO_3$, 10wt% $AgNO_3$ and 50wt% $AgNO_3$, respectively. Solutions of $AgNO_3$/PAN were analyzed by measuring the viscosity and conductivity. Ag/PAN nanofibers were characterized by Scanning Electron Microscopy (SEM), Fourier-transform infrared (FTIR), Energy-dispersive X-ray spectroscopy (EDX) and X-ray photoelectron spectroscopy (XPS). Thickness, porosity, permeability and pressure drop were also determined. In addition, filtration performance tests, quality factor, and bactericidal activity were evaluated.

Structural and morphological properties

Figure 2 shows Scanning Electron Microscopy (SEM) images and the corresponding size distributions of the nanofibers in order to investigate the morphological features of Ag/PAN nanofibers after electrospinning. The fiber diameters were measured from SEM images using image analysis software (Image J1.29X) according to the procedure used by Bortolassi *et al.* [51]. The fiber size distribution was determined by measuring 100 fibers of each filter media. The bar on the figure shows the measurement distribution, whereas the line is an approximation of the distribution function based on a Gaussian distribution approximation. As shown in Figure 2, the substrate (S) was composed by microfibers of 27 µm of mean fiber diameter. All the produced nanofiber filters show approximately 250 nm of fibers diameter, excepting for the 10AgF nanofiber filter (Figure 2C) which had 400 nm fiber diameters. According to Demirsoy *et al*. [54], AgNPs generally have two different effects on the nanofiber diameter. Firstly, the nanoparticles can increase the fiber diameter due to an addition of new material into the polymer matrix or to the agglomeration of the NPs in the nanofibers. Secondly, nanoparticles can also decrease the fiber diameter because of an increase of conductivity of the jet during the electrospinning leading to thinner nanofiber. In our case, we can assume that the addition of AgNPs caused first an increase of fibers diameter for the 10AgF filter following by a decrease of the diameter for the 50AgF fibers filter due to the influence of the conductivity and the viscosity of the solutions.

In order to confirm this assumption, solution conductivity was measured with different amounts of $AgNO_3$. The values of conductivity obtained were 0.09, 0.18, 0.50 and 2.11 mS/cm for 0AgF, 1AgF, 10AgF and 50AgF, respectively. The solution viscosity could be also responsible for the change of the electrospun nanofibers development. The measured viscosity for 0AgF was 471 cP (25^oC) while 933 cP was obtained for the 50AgF solution. We should notice here that a very high viscosity results in the hard ejection of jets from solution [55]. In conclusion, the conductivity and the viscosity are much higher for 50AgF filter causing thinner and lighter fibers layers deposition in comparison to the 10AgF Filter. The solution viscosity of 1AgF and 10AgF were also measured to be 475 cP and 522 cP, respectively. We can assume here that the competition between viscosity and conductivity is responsible for the increase of the diameter of the electrospun nanofibers for the 10AgF filter in comparison to 0AgF, 1AgF, and 50AgF filters.

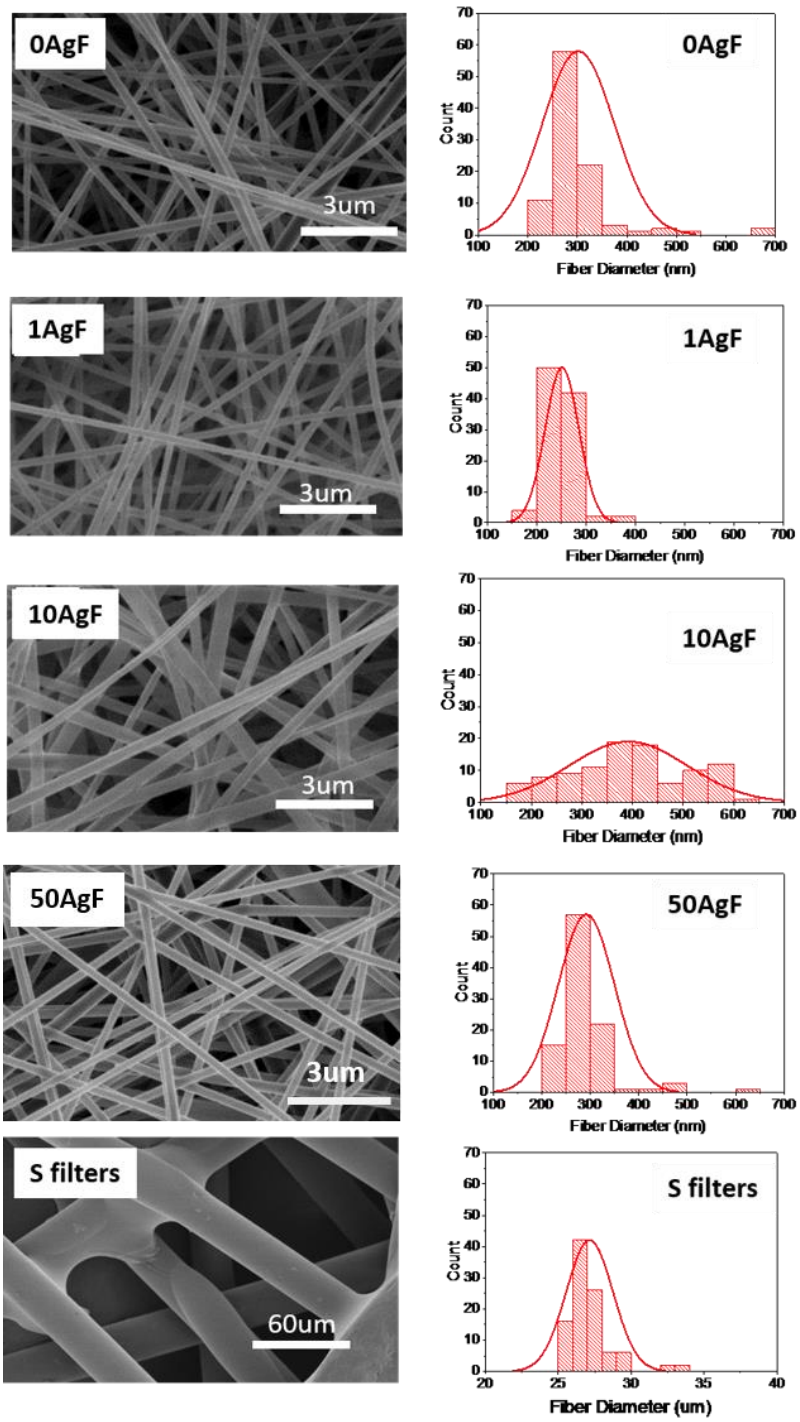

Figure 2 - SEM images electrospun fibers and S filters

The average nanofibers diameter, thickness and basis weight are presented in Table 1. No significant changes are identified in the thickness of the filters when the electrospun nanofibers were added to the substrate because the deposited layer was very thin. Samples were weighted after electrospinning and it was noticed that increasing the amount of AgNPs lower was the sample weight. This could be induced by the increase of the solution viscosity when AgNO3 is added to the solutions resulting in the decrease of the number of nanofibers deposited on the substrate.

Table 1 - Characterization of Ag/PAN fibrous filters and substrate

Samples	Mean fiber diameter (nm)	Thickness (mm)	Basis weight (g/m2)
0AgF	301±7	0.20±0.01	75.08±3
1AgF	251±3	0.18±0.01	75.50±5
10AgF	391±12	0.18±0.01	62.09±1
50AgF	292±6	0.17±0.01	62.53±4
S	27000±0	0.16±0.01	61.07±1

FTIR spectroscopy was used to identify the presence of functional groups on Ag/PAN nanofibers. Figure S2 shows FTIR spectra of PAN nanofibers without and with silver nanoparticles in the range of 4000-700 cm^{-1}. FTIR spectra of PAN fibers display characteristic peaks such as the stretching vibration of nitrile groups (-CN-) at 2240 cm^{-1} and methylene (-CH_2-) at 2930 and bending vibration of methylene (-CH_2) at 1450 cm^{-1} and methyl (-CH_3) in CCH_3 at 1369 cm^{-1} [46]. No significant difference is observed when silver nanoparticles were introducing inside the nanofibers.

An Energy dispersive X-ray spectroscopy (EDX) of Ag/PAN nanofibers recorded along with elemental analysis is presented in Table 2. The EDX analysis reveals the atomic percentage of Ag for the above-described fibers. The results show an increase of silver atomic percentage with the increase of $AgNO_3$ into the PAN solution. Figure S3 shows elemental mapping images of 1AgF, 10AgF, and 50AgF filters. The particles are also evenly distributed over the entire area of the sample confirming the good dispersion of Ag particles in PAN nanofibers. Based on these data, Ag/PAN nanofibers were successfully fabricated and deposited in PET substrate using the electrospinning method to produce air filters. We can notice in Table 2 that the atomic percentages of silver in the obtained filters are much lower than the percentages introduced in the experimental section. This observation could be related to the big contribution of the substrate (made of Polyethylene terephthalate (PET) fibers) to the elemental composition measured by EDX due to the thin film of Ag NPs/PAN nanofibers deposited by electrospinning (on the substrate) and to the high porosity of these deposited films.

Table 2 - EDX data showing the composition of nanofibers filter as well as the substrate

	Atomic Percentage			
Samples	Ag	C	N	O
0AgF	0±0	74±1	23±1	2±1
1AgF	<1	73±1	20±1	6±1
10AgF	<1	70±1	24±1	5±1

50AgF	3±1	61±1	26±1	10±1
S	0±0	63±4	2±1	17±5

XPS was also used to analyze the reduction of AgNPs in PAN nanofibers. First, the surface of PAN filter was evaluated (Figure 3A). The results show the fully scanned spectra in the range of 0-1100 eV from a 500 µm diameter. The background signal was removed using the Shirley (1972) method. The surface atomic concentrations were determined from photoelectron peaks areas using atomic sensitivity factor reported by Scofield [59]. Binding energies (BE) of all core levels were referred to the C-C of C 1s carbon at 284.72 eV. 50AgF electrospun nanofibers were also analyzed in the same conditions (Figure 3B). The overview spectra demonstrate that C, Ag, O, and N atoms are present in the Ag NPs/PAN nanofibers. Figure 3C shows the photoelectron spectrum of Ag 3d. Two peaks are detected at 368.25, 374.25 eV correspond to Ag 3d5/2 and Ag 3d3/2 binding energies, respectively [60-62]. Therefore, the XPS results confirmed that Ag+ ions initially present in Ag/PAN solution was reduced to Ag metallic nanoparticles using DMF/PAN solution. Silver concentration in the electrospun fibers were quantified using AAS (Table S1), which are found to be 0, 57.4 and 287.6 mg/g of electrospun fibers for 0AgF, 10AgF and 50AgF samples respectively.

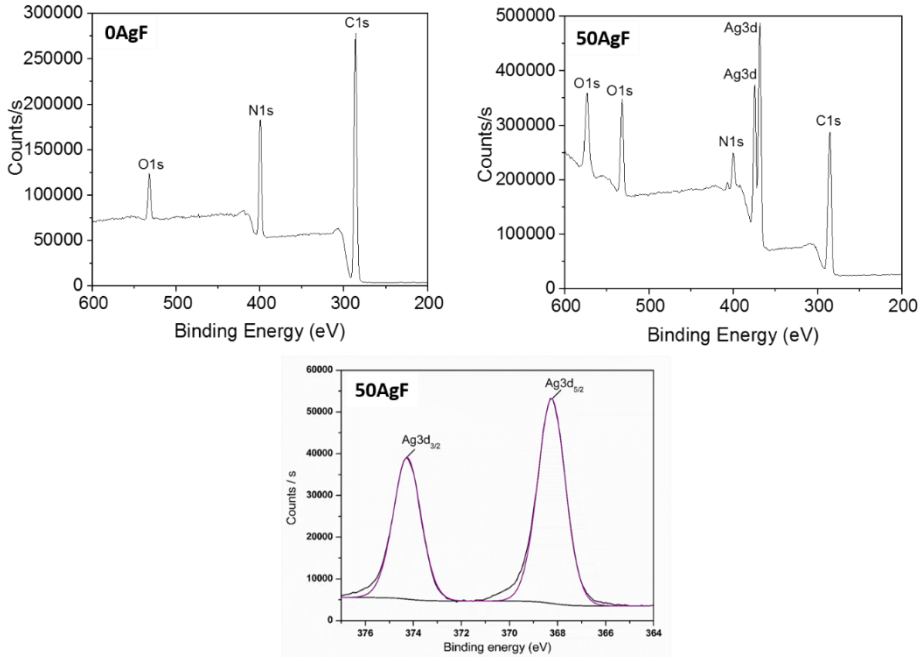

Figure 3 - XPS patterns for the Ag NPs/PAN nanofibers: (A)0AgF and (B)50AgF. (C) XPS pattern of 50AgF in the range of 385-355eV

Distribution of nanoparticles in the PAN electrospun fibers was observed using TEM analysis and shown in Figure 4 (a, b). The distributions of silver nanoparticles are marked using the arrows (Figure 4b inset images) and higher magnification TEM images of 0AgF and 10AgF were provided in the Figure S4. TEM image of 10AgF shows that the silver nanoparticles are distributed uniformly throughout the fibrous matrix. However, silver nanoparticles distributed on the surface of the fibers were mainly playing a key role

in the antibacterial activity of the electrospun mats. Histogram of silver nanoparticles size distribution were provided (inset image of Figure S4) and shows that the silver nanoparticles are below 5 nm. Silver nanoparticles are below 5 nm in size and are uniformly distributed throughout the fibrous matrix. Mechanical properties such as Young's modulus, tensile stress at break and tensile strain at break were calculated and shown as well in Figure 4 (c, d, e). The results obtained from a minimum 7 trials were averaged and reported. Young's modulus was calculated from the linear elastic region of the stress-strain curve. We note here that the size of the electrospun fibers is an important parameter that contributes to the mechanical properties of the electrospun mats. SEM images (Figure 2) evidenced that 0AgF and 50 AgF display no significant difference in their fiber diameter, for this reason, these 2 samples were chosen in order to compare their mechanical properties. Young's modulus and tensile stress at the break for 50AgF sample were improved significantly in comparison to 0AgF sample which proves again that the silver NPs are well dispersed inside the PAN nanofibers and they are involved in the effective reinforcement of the polymer matrix. We noted here that the filter maintains the structural stability during filtration tests.

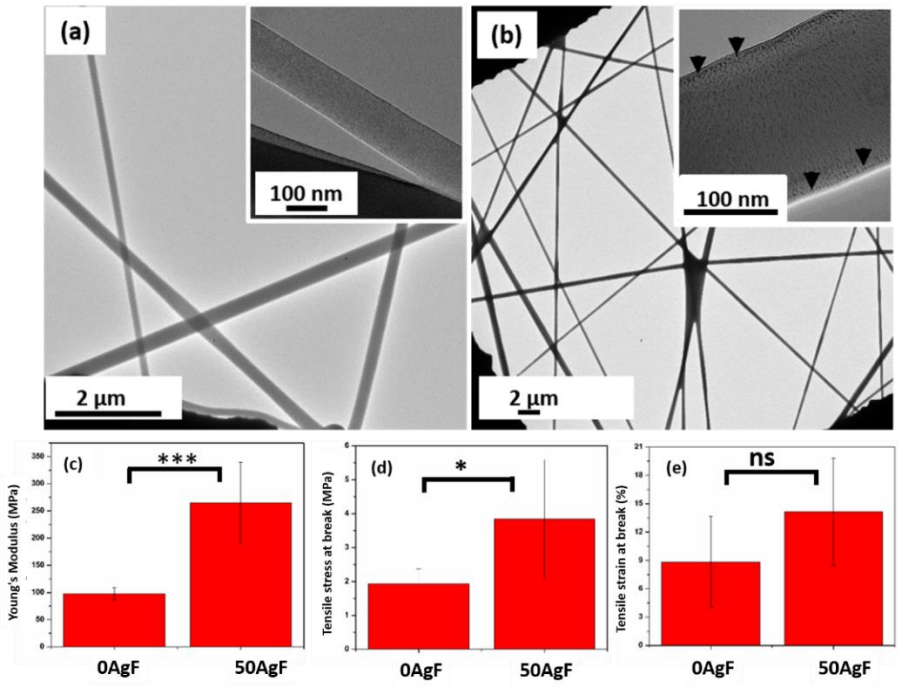

Figure 4 - TEM images of (a) 0AgF, (b) 10AgF (inset images are higher magnification images of the electrospun fibers) (black arrow indicates the silver nanoparticles) and Mechanical properties, (c) Youngs modulus, (d) Tensile stress at break and (e) tensile strain at break of electrospun fibers ($p<0.05$=*, $p<0.0005$=***, ns= no significance)

The crystallinity of the silver nanoparticles was also analyzed using X-ray diffraction analysis and are shown in Figure S1. The peak of 0AgF observed at 17° corresponds to (110) plan of PAN. Crystalline peak corresponds to silver nanoparticles were absent in all samples (1AgF, 10AgF, and 50AgF) which is due

to the small size (<5nm) of silver nanoparticles. In the following section, pressure drop and permeability of the filters will be characterized.

Permeability and pressure drop of nanofiber filters

One way to make the air filter more efficient in filtering out aerosol is to make it more permeable by reducing the pressure drop. The superficial velocity was varied from 0.3 to 3 cm/s and the pressure drop (ΔP) of 0AgF, 1AgF, 10AgF, 50AgF as well as the substrate S was measured using a digital manometer (Figure). It is possible to note that the substrate used (S) has no significant effect on the pressure drop. Therefore, the mats used do not interfere with the performance of the filter.

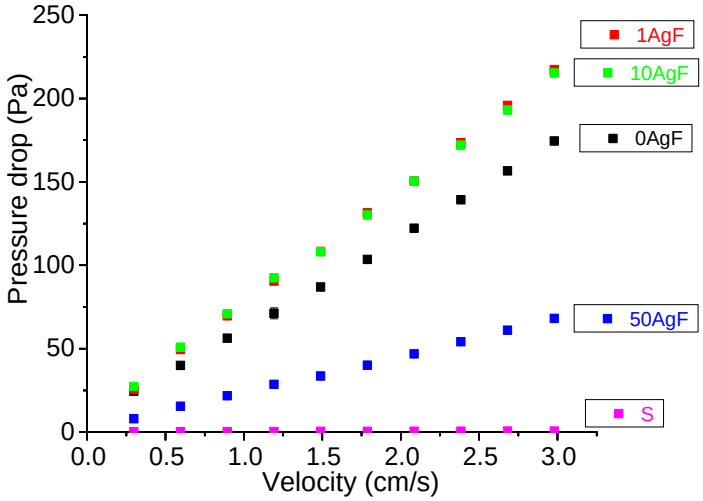

Figure 5 - Pressure drop versus velocity of electrospun filters

The deposition of PAN nanofibers (0AgF) by electrospinning will raise the pressure drop. This could be attributed to the fact that increasing the nanofiber layers on the substrate will decrease the void space hindering the air flow through the filter. The addition of AgNPS to the PAN nanofibers will cause a further increase of the pressure drop for the 1AgF and 10AgF filter. In fact, as demonstrated before, the increase of silver amount in the solution will lead to a rise in the viscosity, which then increases the chain entanglement among the polymer chains. These chain entanglements overcome the surface tension and ultimately result in uniform beadless electrospun nanofibers [56]. This explains the higher-pressure drop for 1AgF and 10AgF comparing to 0AgF.

On the contrary, 50AgF filter had lower pressure drop (68Pa) when compared to 0AgF, 1AgF and 10AgF filters. Fong *et al.* [24] proposed that fiber formation is dependent on the balance of forces caused by surface tension, density of net charges on the jet, and solution viscosity. The solution viscosity is the root cause of changes to the electrospun fiber morphology [57]. It can be also mentioned that increasing Ag

concentration (0 to 50%) consequently changes the solution viscosity (471 to 933 cP). Therefore, 50AgF filter had lower pressure drop due to its high Ag concentration in solution resulting in low nanofibers deposition rate on the collector (as explained in the previous section). In fact, increasing the concentration beyond a critical value will hinder the solution flow through the needle tip [58]. Consequently, 50AgF has a higher permeability constant (k_1) comparing to the other filters due to the lower pressure drop of this filter at 0.03 m/s ( ). Therefore, the air passed through 50AgF filter easier and had lower pressure drop (68Pa). This result suggests that a large increase of nanoparticles concentration into PAN solution decreases the pressure drop such as the aforementioned [21], [59].

Table 3 - Permeability constant of electrospun filters

Samples	K1 (m^2)
0AgF	$6.11E^{-13}$
1AgF	$4.58E^{-13}$
10AgF	$4.58E^{-13}$
50AgF	$1.83E^{-12}$
S	$1.46E^{-10}$

Pressure drop at 0.03 m/s and porosity measured by a digital manometer and Ergun Equation, respectively, are presented in Table 4. According to classic filtration theory, lower superficial velocity is used in air filtration experiments due to diffusion capture mechanism of small particles at this velocity. Porosity measured by theory is related to pressure drop, thickness, superficial velocity, and fiber diameter. Permeability constant and porosity values obtained in this work are in agreement with those reported by Barhate et al. [19]. They investigated the structural and transport properties of an electrospun membrane in relation to the processing parameters in order to understand the distribution, deposition, and orientation of nanofibers in the nanofibrous filtering media. They also used Darcy's equation to measure permeability. Porosity was estimated by the weight and volume of the sample. Even using a different method from them, similar porosity (≈96%) was obtained when added a different amount of AgNPs to PAN solution.

Table 4 – Pressure drop and porosity of electrospun filters

Samples	ΔP at 0.03 m/s	Porosity

	(Pa)	(Ergun Eq.) (%)
0AgF	174.50±0.25	96.81±0.00
1AgF	217.33±0.17	97.05±0.00
10AgF	215.23±0.12	95.51±0.00
50AgF	68.13±0.18	97.88±0.00

Filtration performance of nanofiber filters

Nanoparticles distribution were generated from 5 g/L of NaCl solution in the range of 9 to 300 nm using atomizer aerosol generator and achieved the same standard particle size distribution curve for both filters analyzed (Figure).

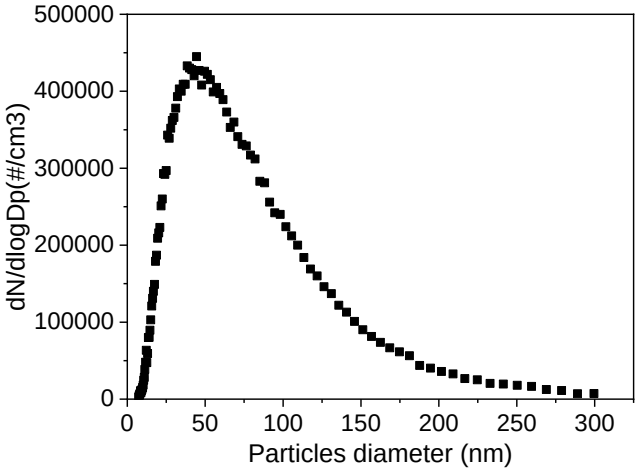

Figure 6 – Nanoparticles distribution using NaCl solution

There are many studies related to the bactericidal activity of Ag/Polymer but no one linked to air filtration.

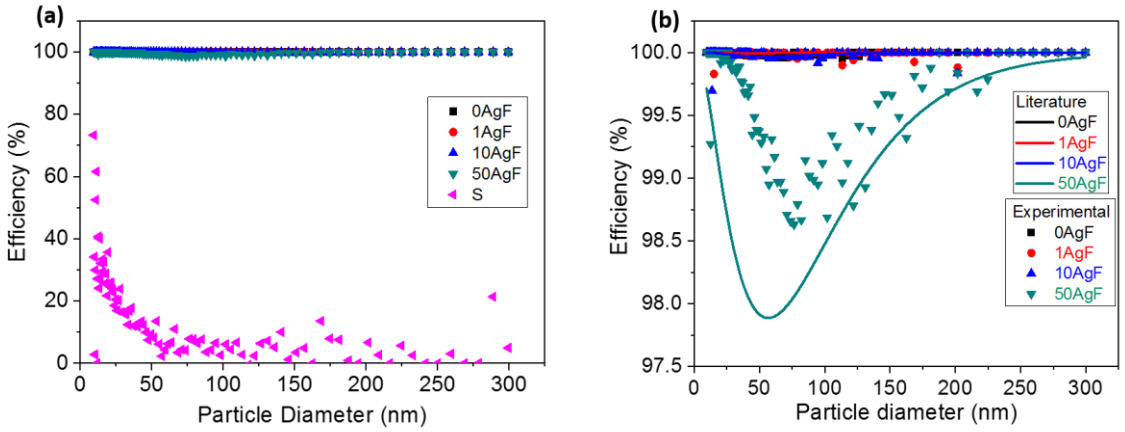

Figure A shows the efficiency to remove nanoparticles (9 – 300 nm) from the air using PAN (0AgF), 1wt% Ag/PAN (1AgF), 10wt% Ag/PAN (10AgF), 50wt% Ag/PAN (50AgF) filters as well as the substrate (S) measured by the following equation:

$$\eta = \frac{C_{up} - C_d}{C_{up}} \quad (05)$$

Particle analyzer of electric mobility coupled to the filtration line was used to measure the concentration of nanoparticles upstream (C_{up}) and downstream (C_d) of the filter medium.

As confirmed by

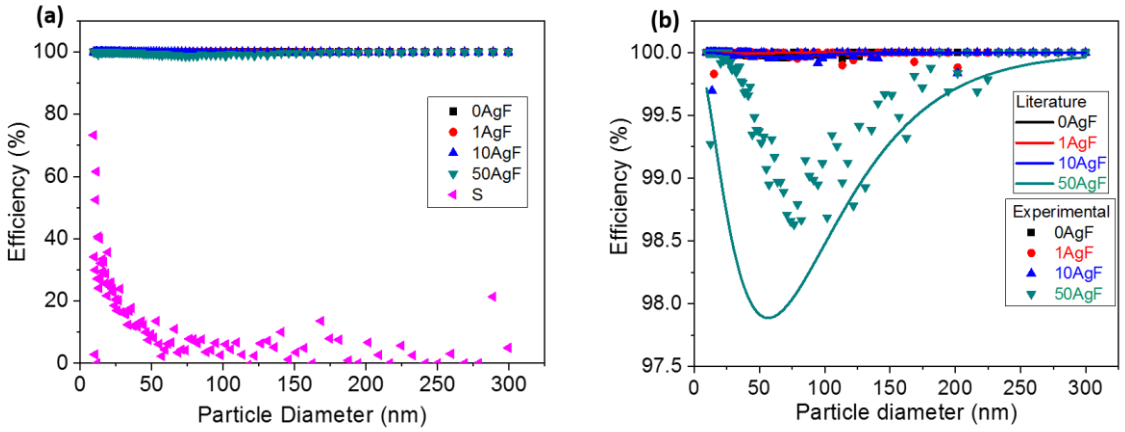

Figure A, the efficiency of the substrate is very low that is why it is used just as a support for the Ag/PAN nanofibers and there is no significant influence in the filtration efficiency. Traditional air filtration media (micrometer-scale fibers), such as glass fibers, spun-bonded fibers, and melt-blown fibers were reviewed by Zhu *et al.* [60] and showed low filtration efficiency for fine airborne nanoparticles (0.1 - 0.5 μm) because the

pores size formed with micrometer-scale fibers are fairly large [58 - 59]. Although some nonwoven filtration materials exhibit good filtering performance for micrometer-level particles, their performance is still far from satisfactory for sub-micrometer PM and for bacterial filtration. To improve the filtration efficiency of the traditional filter media, it is necessary to create thicker media. The filtration efficiency of common fibrous filter grows with the increase of layers deposition, which is directly proportional to the air pressure drop. This explains the fact that 0AgF, 1AgF and 10AgF filter got a higher filtration efficiency (≈100%) and also higher air pressure drop (≈200 Pa). Thus, in order to achieve high filtration efficiency, a higher pressure drop is inevitable for general air filters—an effect that causes large energy losses [66-67].

Looking closer from

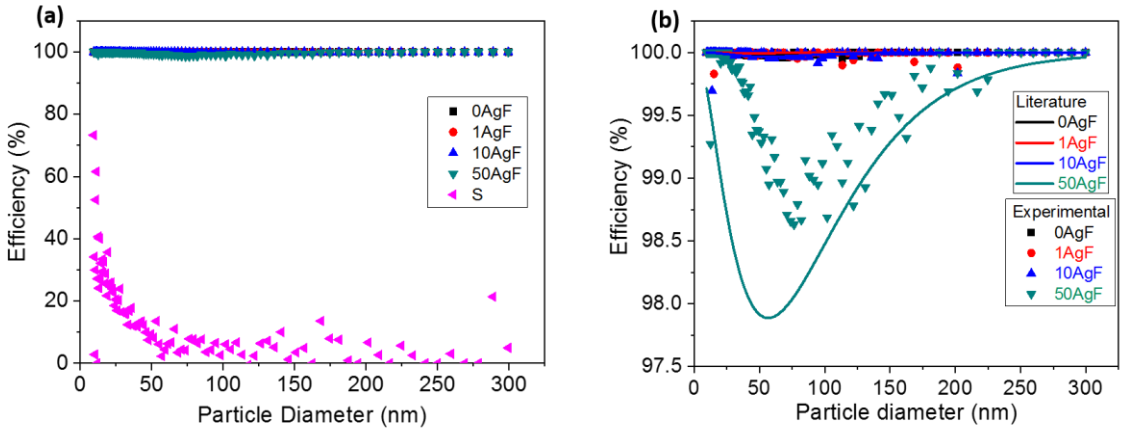

Figure a, it was possible to obtain

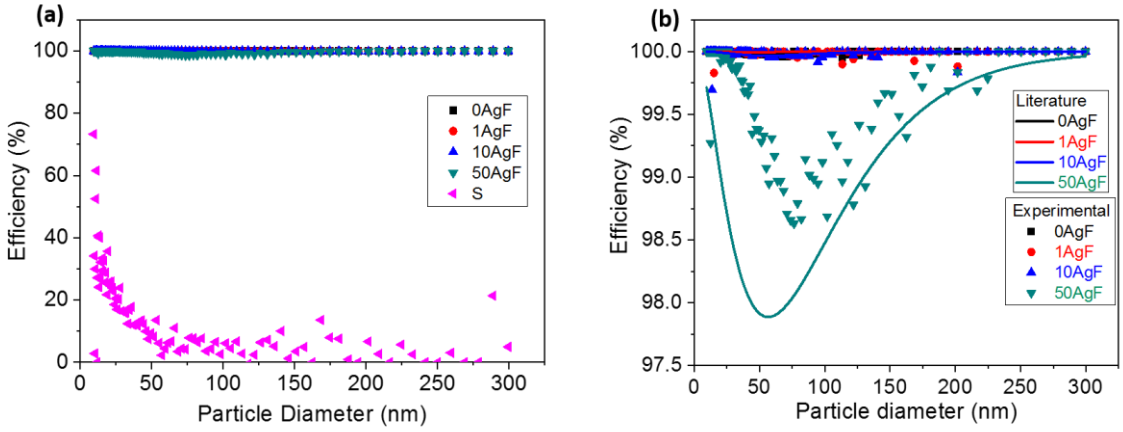

Figure b that represent the filtration efficiency in a different scale for both filter media (0AgF, 1AgF, 10AgF, and 50AgF) comparing to the theory. Therefore, the results show that 50AgF was less efficient compared to the other filters because of the relatively low specific surface area but even that got efficiency above 98.6%. The characteristic penetration curve of 50AgF is similar to the total curve of various filtration mechanisms studied by Hinds [52]. Three main mechanisms to determine filter's efficiency versus particle size known

such as interception, inertial impaction, and diffusion were analyzed in order to explain the behavior of the filtration efficiency curves. These mechanisms were also reviewed by Lv *et al.* [65] to evaluate the filtration efficiency of the electrospun filters. Large particles above 0.4 µm in diameter will be captured due to both impaction and interception mechanisms. Generally, medium particles in the 0.1 to 0.4 µm diameter range are considered as the most penetrating and are captured by both diffusion and interception filtration mechanisms. Small particles below 0.1 µm in diameter are captured by the diffusion mechanism. A fibrous filter is generally less effective at removing particles in the 0.1 µm to 0.4 µm particle diameter range. Particles between this range are therefore too large for effective diffusion and too small for inertial impaction and interception, hence the filter's efficiency drops within this range [66]. This can also be used to measure the total collection efficiency of the filter media of European Standard by summing diffusion, interception, inertial and gravitational mechanisms. Diffusion is predominant among the collection mechanisms. It is possible to note that experimental efficiency curve is very similar to the literature efficiency curve from Hinds [52]. A small deviation is related to the parameters used to measure the efficiency such as fiber and particle diameter, thickness and porosity.

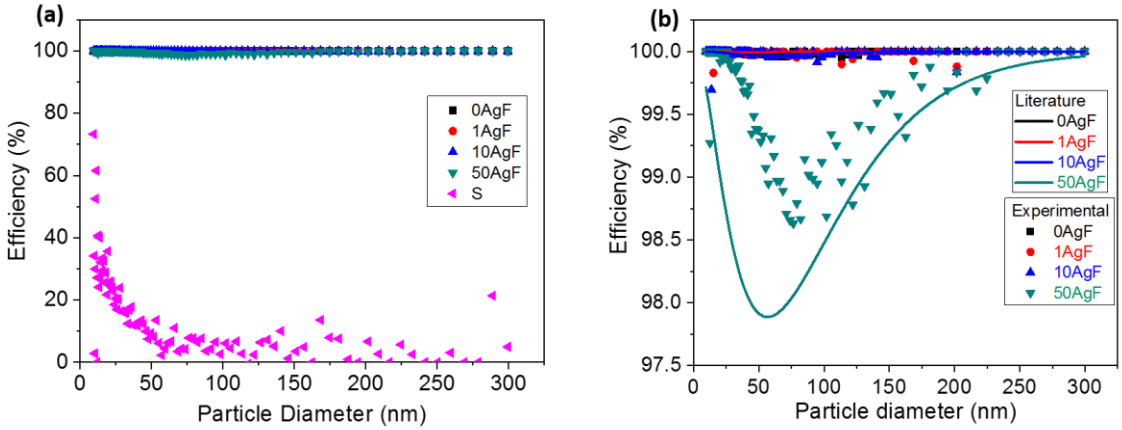

Figure 7 – a) Efficiency of different filter media and b) Comparison between experimental and theoretical efficiency

Quality factor (Q_F) is another factor to analyze the performance of the filter media and the values related to 100 nm particles diameter are shown in Table 5. Higher Q_F means a filter with great filtration efficiency and lower pressure drop. For this reason, 50AgF had the highest Q_F as a result of the lower pressure drop (68Pa) and also great efficiency (>98.65%) to remove nanoparticles (9-300 nm) from the air.

Table 5 – Quality factor of different filters

Samples	Quality factor (Pa^{-1})
0AgF	0.05

1AgF	0.04
10AgF	0.04
50AgF	0.06

A limited number of studies based on filtration theory have already investigated the quality factor effect of nanofibers filters [17], [71-73]. Comparing these studies, it is possible to note that the filters reported in this study are composed of PAN material of small fibers diameter that probably explains the high-quality factor. In addition, a very high filtration efficiency (approximately 100% filtration efficiency) in the range of 9 to 300 nm aerosol particles diameters and quality factor (0.05) were reached by our PAN/Ag NPs filter in comparison to commercial filters (filtration efficiency less than 80% and quality factor of 0.02) reported elsewhere [17], [70], [71]. It should be noted that the face velocity, particle size, and material composition may be different in the aforementioned studies. Therefore, caution should be exercised when comparing the data. Wang *et al*.[9] reported high filtration efficiency (99.972%), low pressure drop (57 Pa), satisfactory quality factor (0.14 Pa^{-1}). However, 300-500 nm mass-average particular particle size was used in their study. Usually, it is easier to remove microparticles from the air when comparing to nanoparticles. Another difference in this work is that nanoparticles in the range of 9 to 300 nm were used. This particle size is the most difficult to remove besides it causes many diseases. This work highlights great results of quality factor (0.05 Pa^{-1}) even using nanoparticles to simulate air contamination. Filter media reached similar quality factor compared to other studies with PAN filters even adding Ag nanoparticles to PAN nanofibers. Moreover, the filters produced in this work, besides to be efficient to remove nanoparticles, can also avoid bacteria growing.

According to European Union Standard for both HEPA and ULPA filters — EN 1822 [72], 0AgF filter media could be easily promoted as H13 (High-Efficiency Particulate Air Filters - HEPA > 99.95% collection efficiency), 1AgF and 10AgF as E12 (Efficiency Particulate Air Filters – EPA > 99.5% collection efficiency) and 50AgF as E11 (EPA > 95% collection efficiency). As stated by ISO Cleanroom Standards, 0AgF, 1AgF, and 10AgF are classified as ISO Class 3, and 50AgF as ISO Class 4 because exceeded the limits of the maximum concentration (1000 particles/m^3 of air) for particles of 0.1 µm in diameter.

Bactericidal activity

In order to assess the antibacterial properties of Ag/PAN nanofiber surfaces, agar contact tests were first carried out with 1AgF and PAN solely (Table 6).

Table 6 – Agar contact test

Test	Colonies (CFU)

Blank	87 ± 10
PAN	25 ± 12
1AgF	0 ± 1

Results of Table 6 evidence a colony decrease for PAN solely (25 *vs* 87). As PAN alone was not reported to have bactericidal activity, bacterial adsorption onto the PAN pieces is thus supposed. Moreover, the 1AgF surface was able to deactivate nearly all the bacteria that were put in contact with the material after 6 h-contact; over the triplicates, only a trial exhibited a colony whereas the two others showed no colonies. This result underlines the efficient bactericidal activity of the Ag/PAN nanofibers that contains the lowest Ag content tested (1wt% Ag/PAN).

Liquid bactericidal tests were also carried out to (i) expose the material to higher bacterial concentrations (up to 10^8 CFU/mL) and (ii) to assess silver nanoparticle release from the material. Figure shows antibacterial results obtained for Ag/PAN filters when compared to PAN filters and blanks without materials. It is worth noticing that log removal values can be considered significantly different if a difference of at least 1 log is observed between two values. The results evidence that PAN has no bactericidal effect when compared to blank whatever the bacterial concentration tested (either 10^8 or 10^4 CFU/mL). Conversely, Ag/PAN filters showed total removal of 10^4 CFU/mL for all the silver contents implemented, indicating that the nanofibers are endowed with efficient antibacterial properties due to the introduction of Ag nanoparticles. We should notice here that against 10^8 CFU/mL, only 50AgF deactivated all the bacteria. This result is consistent with the fact that antibacterial action depends on key factors: nature and concentration of the antibacterial agent, bacteria type and concentration, and contact time between the bacteria and the antibacterial agent. So, 50AgF is more efficient than the other filters when the higher concentration was used (10^8 CFU/ml) due to the highest Ag concentration.

Atomic Absorption Spectroscopy (AAS) was done to assay total Ag concentration in the suspensions that were recovered after 5 h-bactericidal tests. Figure 9 gives the concentrations measured. As demonstrated by XPS analyses, silver was reduced to Ag(0) and the silver released is thus expected to be silver metallic nanoparticles (AgNPs). Samples were either analyzed directly or pre-filtrated over 0.2 µm-filter. Whatever the material, Figure 9 shows that the filtration step has no incidence on the concentrations measured, meaning that AgNPs have diameters lower than 200 nm. This result is in accordance with SEM images (Figure 2) where AgNPs were not visible, probably due to the fact that these nanoparticles have diameters lower than 50 nm.

For 1AgF and 10AgF materials, the silver concentration does not exceed 0.13 mg/L (i.e. 1,3 µg), suggesting that the material surface should be mainly responsible for the biocide effect. Moreover, the concentration released remains very close to the upper silver limit authorized in drinking waters (i.e. 0.1 mg/L) [74], which opens ways to new applications for these filters. For 50AgF nanofibers, the silver

concentration is much more important (about 2.4 mg/L), which does not exclude an antibacterial action coming from the released AgNPs in addition to the surface one.

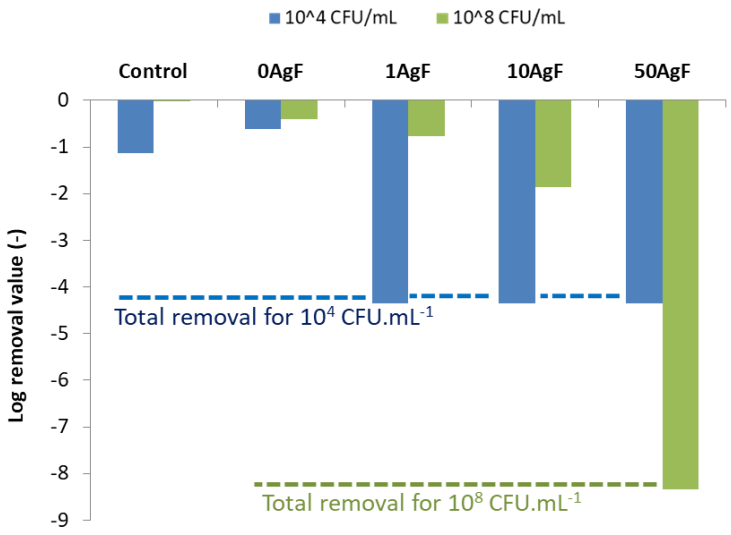

Figure 8 - Liquid bactericidal tests: log removal values obtained against *E.coli* after 5 h-contact

The log-removal is defined as the logarithm (base 10) ratio of the bacterial concentration C(CFU/mL) measured after 5 h-reaction to the initial bacterial concentration C_0 (CFU/mL). A log-removal value of -log (C_0) is attributed to the particular case of total removal. One log removal, which corresponds to a bacterial reduction of 90%, is usually admitted as the minimal value allowing to evidence a biocide effect [73]

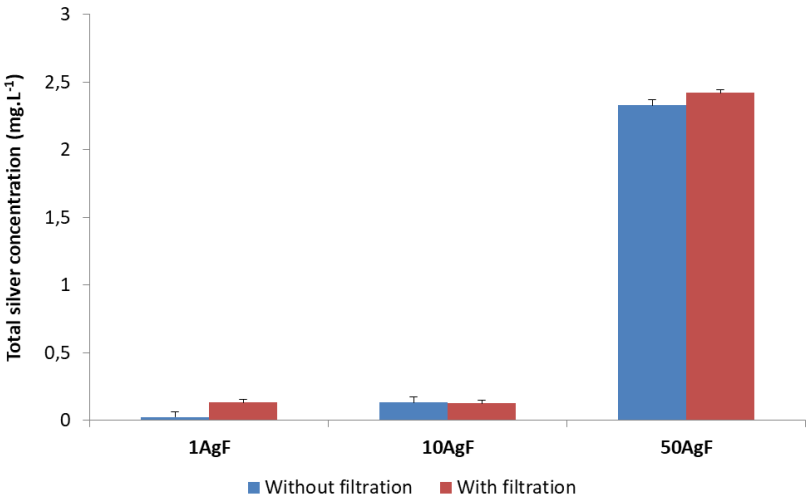

Figure 9 - Total silver concentrations measured in the bacterial suspensions that were recovered after 5 h of bactericidal tests carried out with different Ag/PAN nanofiber filters. Analyses were performed by AAS and prior silver solubilization was performed by suspension acidification that was done either directly or after a filtration step on a cellulose acetate membrane (0.2 µm-pore sizes)

We should note here that antibacterial action depends on a wide range of factors, including nature, size, shape, and concentration of the antibacterial agent [75], [76]. It is also important to analyze the type and concentration of the bacteria and contact time between the bacteria and the antibacterial agent [77]. Smaller size nanoparticles (<5 nm) of spherical shape display high surface area compared to large size particles (above 50 nm) and facilitates the antibacterial activity [75]. Lv *et al.* [78] showed for instance antibacterial activity of the electrospun nanofibrous membranes loaded with small size nanoparticles. However, literature results on silver nanoparticles shape dependent antibacterial activities are inconsistent. Kim *et al.* provided antibacterial activity of different shape of silver nanoparticles. They demonstrate that the antibacterial activity will decrease as follows: plates > spheres >cubes [76]. However, Pal et al. [79] demonstrated that truncated triangular silver nanoparticles are better than spherical and rod-shaped silver nanoparticles. In this study, silver nanoparticles have a spherical shape and a diameter smaller than 5 nm which are advantageous to improve the antibacterial activity.

From the obtained results, the significant improvement of filtration performance reveals that the deposition of AgNPs in PAN solution to produce electrospun nanofibers is an efficient way to enhance the fibrous filter media, which can meet the requirement of an efficient filter to remove nanoparticles from the air and to be used as a bactericidal material as well. The results show that 1AgF and 10AgF had similar data of porosity, permeability and filtration efficiency as well as antibacterial activity. 50AgF has the lowest pressure drop and the highest porosity and permeability. However, this filter media has lower filtration efficiency (>98.6%) comparing to the other filters (≈100%). Moreover, 50AgF exhibits the highest bactericidal activity when 10^8 CFU/ml initial bacterial concentration was used but high AgNPs release was observed.

Conclusions

Electrospinning was shown to be effective nanotechnology to successfully prepare Ag/PAN electrospun nanofibers with different concentrations of $AgNO_3$ in the solution. Viscosity and conductivity went up when increased AgNPs in the solution. XDR, TEM, FTIR, EDX, XPS, SEM images demonstrated the formation of Ag nanoparticles and their uniform dispersion in the nanofiber filters. Ag/PAN filters were also characterized by a thickness, porosity, pressure drop, and permeability, and showed that the air can easily pass through the filter with low-pressure drop. The results showed that 1AgF and 10AgF had similar data of porosity (96%), permeability ($4.58E^{-13}m^2$), filtration efficiency (≈100%), quality factor (0.04 Pa^{-1}) and bactericidal activity against 10^4 CFU/ml initial bacterial concentrations (100%). Therefore, comparing these two filters, adding just 1wt%$AgNO_3$ in PAN solution was sufficient to achieve great filtration efficiency and antibacterial activity, in addition to its lowest price due to less quantity of AgNPs used. However, the filters had a lower pressure drop and higher permeability when 50%AgNPs were added in PAN solution. This filter media had the lowest filtration efficiency (>98.6%) comparing to filters

aforementioned but even so, 50AgF had a great efficiency to remove nanoparticles from the air which is considerate as E11 (EPA > 95% collection efficiency) according to EN 1822 [72]. Nevertheless, 50AgF had the highest quality factor which means that this filter had low-pressure drop and high filtration efficiency. In general, filters achieved high efficiency (≈100%) to remove nanoparticles in the range of 9 to 300 nm and high-quality factor (≈0.05 Pa^{-1}) even adding Ag nanoparticles to PAN nanofibers. 50AgF was highly efficient to kill bacteria when 10^8 CFU/ml initial bacteria concentrations were used. Then, the resultant Ag/PAN nanofibers showed excellent antibacterial activity depending on the initial *E. coli* bacteria concentrations. Our finding suggests that Ag/PAN nanofiber media could be widely applied in air filtration applications to remove nanoparticles from the air and also efficient to deactivate bacteria. These filters were developed to be resistant, economic and could be produced in large scale. They could be used as individual protection (masks), cleanroom (biomedical, electronics, pharmaceutical, automotive) and indoor air purification (airline cabin).

Acknowledgments

The authors would like to thank the National Council of Technological and Scientific Development (CNPq), Coordination for the Improvement of Higher Education Personnel (CAPES - Fincance Code 001), São Paulo Research Foundation (FAPESP) grand number (2016/20500-6) for their financial support, Freudenberg Group for supply membranes and Prof. Rosário E. S. Bretas (DEMa – UFSCar) for helpful advice. The authors would like to thank as well Dr. Jonathan Barès (Laboratoire de Mécanique et Génie Civil) for mechanical tests.

References

[1] M. He *et al.*, "Differences in allergic inflammatory responses between urban PM2.5 and fine particle derived from desert-dust in murine lungs," *Toxicol. Appl. Pharmacol.*, vol. 297, pp. 41–55, 2016.

[2] X. Li and Y. Gong, "Design of Polymeric Nanofiber Gauze Mask to Prevent Inhaling PM2.5 Particles from Haze Pollution," *J. Chem.*, vol. 2015, pp. 1–5, 2015.

[3] X. Yao *et al.*, "The water-soluble ionic composition of PM2.5 in Shanghai and Beijing, China," *Atmos. Environ.*, vol. 36, no. 26, pp. 4223–4234, 2002.

[4] C. Cao *et al.*, "Inhalable Microorganisms in Beijing ' s PM 2.5 and PM 10 Pollutants during a Severe Smog Event," *Environ. Sci. Technol.*, vol. 48, pp. 1499–1507, 2014.

[5] R. Givehchi and Z. Tan, “The effect of capillary force on airborne nanoparticle filtration,” *J. Aerosol Sci.*, vol. 83, pp. 12–24, 2015.

[6] N. Vinh and H.-M. Kim, “Electrospinning Fabrication and Performance Evaluation of Polyacrylonitrile Nanofiber for Air Filter Applications,” *Appl. Sci.*, vol. 6, no. 9, p. 235, 2016.

[7] R. S. Barhate and S. Ramakrishna, “Nanofibrous filtering media: Filtration problems and solutions from tiny materials,” *J. Memb. Sci.*, vol. 296, no. 1–2, pp. 1–8, 2007.

[8] A. Udo and G. Kreck, “Breve introdução à Tecnologia de Salas Limpas : enfrentando os desafios futuros,” *SBCC*, pp. 32–38, 2013.

[9] Z. Wang, Z. Pan, J. Wang, and R. Zhao, “A novel hierarchical structured poly(lactic acid)/titania fibrous membrane with excellent antibacterial activity and air filtration performance,” *J. Nanomater.*, vol. 2016, 2016.

[10] G. Duan, H. Fang, C. Huang, S. Jiang, and H. Hou, “Microstructures and mechanical properties of aligned electrospun carbon nanofibers from binary composites of polyacrylonitrile and polyamic acid,” *J. Mater. Sci.*, vol. 53, no. 21, pp. 15096–15106, 2018.

[11] S. Jiang, D. Han, C. Huang, G. Duan, and H. Hou, “Temperature-induced molecular orientation and mechanical properties of single electrospun polyimide nanofiber,” *Mater. Lett.*, 2017.

[12] L. Huang, J. T. Arena, S. S. Manickam, X. Jiang, B. G. Willis, and J. R. Mccutcheon, “Improved mechanical properties and hydrophilicity of electrospun nanofiber membranes for filtration applications by dopamine modification,” *J. Memb. Sci.*, vol. 460, pp. 241–249, 2014.

[13] X. Wang, B. Ding, G. Sun, M. Wang, and J. Yu, “Electro-spinning/netting: A strategy for the fabrication of three-dimensional polymer nano-fiber/nets,” *Prog. Mater. Sci.*, vol. 58, no. 8, pp. 1173–1243, 2013.

[14] N. Wang, X. Wang, B. Ding, and G. Sun, “Tunable fabrication of three-dimensional polyamide-66 nano-fiber/nets for high efficiency fine particulate filtration,” *J. Mater. Chem.*, vol. 22, pp. 1445–1452, 2012.

[15] D. Chen, T. Liu, X. Zhou, W. C. Tjiu, and H. Hou, “Electrospinning fabrication of high strength and toughness polyimide nanofiber membranes containing multiwalled carbon nanotubes,” *J. Phys. Chem. B*, vol. 113, no. 29, pp. 9741–9748, 2009.

[16] S. Jiang, Y. Chen, G. Duan, C. Mei, A. Greiner, and S. Agarwal, “Electrospun nanofiber reinforced composites: A review,” *Polym. Chem.*, vol. 9, no. 20, pp. 2685–2720, 2018.

[17] R. Al-Attabi, L. F. Dumée, J. A. Schutz, and Y. Morsi, "Pore engineering towards highly efficient electrospun nanofibrous membranes for aerosol particle removal," *Sci. Total Environ.*, vol. 625, pp. 706–715, 2017.

[18] J. Matulevicius, L. Kliucininkas, T. Prasauskas, D. Buivydiene, and D. Martuzevicius, "The comparative study of aerosol filtration by electrospun polyamide, polyvinyl acetate, polyacrylonitrile and cellulose acetate nanofiber media," *J. Aerosol Sci.*, vol. 92, pp. 27–37, 2016.

[19] K. M. Yun, C. J. Hogan, Y. Matsubayashi, M. Kawabe, F. Iskandar, and K. Okuyama, "Nanoparticle filtration by electrospun polymer fibers," *Chem. Eng. Sci.*, vol. 62, no. 17, pp. 4751–4759, 2007.

[20] S. Ryu, J. W. Chung, and S. Kwak, "Dependence of photocatalytic and antimicrobial activity of electrospun polymeric nanofiber composites on the positioning of Ag–TiO2 nanoparticles," *Compos. Sci. Technol.*, vol. 117, pp. 9–17, 2015.

[21] R. S. Barhate, C. K. Loong, and S. Ramakrishna, "Preparation and characterization of nanofibrous filtering media," *J. Memb. Sci.*, vol. 283, no. 1–2, pp. 209–218, 2006.

[22] J. Li, F. Gao, L. Q. Liu, and Z. Zhang, "Needleless electro-spun nanofibers used for filtration of small particles," *Express Polym. Lett.*, vol. 7, no. 8, pp. 683–689, 2013.

[23] X. Huang *et al.*, "Hierarchical electrospun nanofibers treated by solvent vapor annealing as air filtration mat for high-efficiency PM2.5 capture," *Sci. China Mater.*, no. August, pp. 1–14, 2018.

[24] H. Fong, I. Chun, and D. H. Reneker, "Beaded nanofibers formed during electrospinning," *Polymer (Guildf).*, vol. 40, no. 16, pp. 4585–4592, 1999.

[25] S. Zhang, W. S. Shim, and J. Kim, "Design of ultra-fine nonwovens via electrospinning of Nylon 6: Spinning parameters and filtration efficiency," *Mater. Des.*, vol. 30, no. 9, pp. 3659–3666, 2009.

[26] A. Patanaik, V. Jacobs, and R. D. Anandjiwala, "Performance evaluation of electrospun nanofibrous membrane," *J. Memb. Sci.*, vol. 352, no. 1–2, pp. 136–142, 2010.

[27] Y. Wang, W. Li, Y. Xia, X. Jiao, and D. Chen, "Electrospun flexible self-standing γ-alumina fibrous membranes and their potential as high-efficiency fine particulate filtration media," *J. Mater. Chem. A*, vol. 2, no. 36, pp. 15124–15131, 2014.

[28] H. K. Lee, E. H. Jeong, C. K. Baek, and J. H. Youk, "One-step preparation of ultrafine poly(acrylonitrile) fibers containing silver nanoparticles," *Mater. Lett.*, vol. 59, no. 23, pp. 2977–2980, 2005.

[29] N. W. Oh, J. Jegal, and K. H. Lee, "Preparation and characterization of nanofiltration composite

membranes using polyacrylonitrile (PAN). I. Preparation and modification of PAN supports," *J. Appl. Polym. Sci.*, vol. 80, no. 10, pp. 1854–1862, 2001.

[30] J. Wang, Z. Yue, J. S. Ince, and J. Economy, "Preparation of nanofiltration membranes from polyacrylonitrile ultrafiltration membranes," *J. Memb. Sci.*, vol. 286, no. 1–2, pp. 333–341, 2006.

[31] J. Sutasinpromprae, S. Jitjaicham, M. Nithitanakul, C. Meechaisue, and P. Supaphol, "Preparation and characterization of ultrafine electrospun polyacrylonitrile fibers and their subsequent pyrolysis to carbon fibers," *Polym. Int.*, vol. 55, pp. 825–833, 2006.

[32] A. Vanangamudi, S. Hamzah, and G. Singh, "Synthesis of hybrid hydrophobic composite air filtration membranes for antibacterial activity and chemical detoxification with high particulate filtration efficiency (PFE)," *Chem. Eng. J.*, vol. 260, pp. 801–808, 2015.

[33] M. Rai, A. Yadav, and A. Gade, "Silver nanoparticles as a new generation of antimicrobials," *Biotechnol. Adv.*, vol. 27, no. 1, pp. 76–83, 2009.

[34] J. S. Kim *et al.*, "Antimicrobial effects of silver nanoparticles," *Nanomedicine Nanotechnology, Biol. Med.*, vol. 3, no. 1, pp. 95–101, 2007.

[35] S. Shrivastava, T. Bera, A. Roy, G. Singh, P. Ramachandrarao, and D. Dash, "Characterization of enhanced antibacterial effects of novel silver nanoparticles," *Nanotechnology*, vol. 18, no. 22, 2007.

[36] S. Lu *et al.*, "Preparation of silver nanoparticles/polydopamine functionalized polyacrylonitrile fiber paper and its catalytic activity for the reduction 4-nitrophenol," *Appl. Surf. Sci.*, vol. 411, pp. 163–169, 2017.

[37] V. K. Sharma, R. A. Yngard, and Y. Lin, "Silver nanoparticles: Green synthesis and their antimicrobial activities," *Adv. Colloid Interface Sci.*, vol. 145, no. 1–2, pp. 83–96, 2009.

[38] P. Rujitanaroj, N. Pimpha, and P. Supaphol, "Preparation, characterization, and antibacterial properties of electrospun polyacrylonitrile fibrous membranes containing silver nanoparticles," *J. ofAppliedPolymer Sci.*, vol. 116, pp. 1967–1976, 2010.

[39] G. N. Sichani, M. Morshed, M. Amirnasr, and D. Abedi, "In Situ Preparation, electrospinning, and characterization of polyacrylonitrile nanofibers containing silver nanoparticles," *J. ofAppliedPolymer Sci.*, vol. 116, pp. 1021–1029, 2009.

[40] J. J. Castellano *et al.*, "Comparative evaluation of silver-containing antimicrobial dressings and drugs," *Int. Wound J.*, vol. 4, no. 2, 2007.

[41] Q. Shi *et al.*, "Durable antibacterial Ag/polyacrylonitrile (Ag/PAN) hybrid nanofibers prepared by

atmospheric plasma treatment and electrospinning," *Eur. Polym. J.*, vol. 47, no. 7, pp. 1402–1409, 2011.

[42] N. L. Lala *et al.*, "Fabrication of nanofibers with antimicrobial functionality used as filters: protection against bacterial contaminants," *Biotechnol. Bioeng.*, vol. 97, no. 6, pp. 1357–1365, 2007.

[43] S. Navaladian, B. Viswanathan, R. Viswanath, and T. Varadarajan, "Thermal decomposition as route for silver nanoparticles," *Nanoscale Res. Lett.*, vol. 2, no. 1, pp. 44–48, 2007.

[44] I. P. Santos, C. S. Rodríguez, and L. M. L. Marzán, "Self-Assembly of Silver Particle Monolayers on Glass from Ag+ Solutions in DMF," *J. Colloid Interdace Sci.*, vol. 221, no. 2, pp. 236–241, 2000.

[45] Y. Liu *et al.*, "Self-Assembled AgNP-containing nanocomposites constructed by electrospinning as efficient dye photocatalyst materials for wastewater treatment," *Nanomaterials*, vol. 8, no. 1, p. 35, 2018.

[46] Y. C. Chu, C. H. Tseng, K. T. Hung, C. C. Wang, and C. Y. Chen, "Surface modification of polyacrylonitrile fibers and their application in the preparation of silver nanoparticles," *J. Inorg. Organomet. Polym.*, vol. 15, no. 3, pp. 309–317, 2005.

[47] A. W. Jatoi, I. S. Kim, and Q. Q. Ni, "A comparative study on synthesis of AgNPs on cellulose nanofibers by thermal treatment and DMF for antibacterial activities," *Mater. Sci. Eng. C*, vol. 98, pp. 1179–1195, 2019.

[48] D. Aragon, M. Sole, and S. Brown, "Outcomes of an infection prevention project focusing on hand hygiene and isolation practices," *AACN Clin Issues*, vol. 16, no. 2, pp. 121–32, 2005.

[49] M. Nasr, R. Viter, C. Eid, R. Habchi, P. Miele, and M. Bechelany, "Enhanced photocatalytic performance of novel electrospun BN/TiO_2 composite nanofibers," *New J. Chem.*, vol. 41, no. 1, pp. 81–89, 2017.

[50] S. Ergun, "Fluid flow through packed columns," *Chem. Eng. Prog.*, vol. 48, no. 2, pp. 889–94, 1952.

[51] A. C. C. Bortolassi, V. G. Guerra, and M. L. Aguiar, "Characterization and evaluate the efficiency of different filter media in removing nanoparticles," *Sep. Purif. Technol.*, vol. 175, pp. 79–86, 2016.

[52] W. C. Hinds, *Aerosol Technology Properties, Behavior and Measure of Airborne Particles*, 2ed ed. New York, 1982.

[53] P. M. Barros, S. S. R. Cirqueira, and M. L. Aguiar, "Evaluation of the Deposition of Nanoparticles in Fibrous Filter," in *Materials Science Forum*, 2014, vol. 802, pp. 174–179.

[54] N. Demirsoy *et al.*, "The effect of dispersion technique, silver particle loading, and reduction method

on the properties of polyacrylonitrile – silver composite nanofiber," *J. Ind. Text.*, vol. 45, no. 6, pp. 1173–1187, 2016.

[55] Z. Li and C. Wang, "Effects of working parameters on electrospinning," in *One-Dimensonal Nanostructures*, 2013, pp. 15–28.

[56] A. Haider, S. Haider, and I. Kang, "A comprehensive review summarizing the effect of electrospinning parameters and potential applications of nanofibers in biomedical and biotechnology," *Arab. J. Chem.*, 2015.

[57] R. M. Nezarati, M. B. Eifert, and E. Cosgriff-Hernandez, "Effects of humidity and solution viscosity on electrospun fiber morphology," *Tissue Eng. Part C*, vol. 19, no. 10, pp. 810–819, 2013.

[58] S. Haider, Y. Al-zeghayer, F. A. A. Ali, M. Imran, and M. O. Aijaz, "Highly aligned narrow diameter chitosan electrospun nanofibers," *J. Polym. Res.*, vol. 20, p. 105, 2013.

[59] P. Zhang *et al.*, "In situ assembly of well-dispersed Ag nanoparticles (AgNPs) on electrospun carbon nanofibers (CNFs) for catalytic reduction of 4-nitrophenol," *Nanoscale*, vol. 3, p. 3357, 2011.

[60] M. Zhu *et al.*, "Electrospun Nanofibers Membranes for Effective Air Filtration," *Macromol. Mater. Eng.*, vol. 302, no. 1, p. 1600353, 2017.

[61] C. H. Hung and W. W. F. Leung, "Filtration of nano-aerosol using nanofiber filter under low Peclet number and transitional flow regime," *Sep. Purif. Technol.*, vol. 79, no. 1, pp. 34–42, 2011.

[62] S. Wang, C. C. Yap, J. He, C. Chen, S. Y. Wong, and X. Li, "Electrospinning: a facile technique for fabricating functional nanofibers for environmental applications," *Nanotechnol Rev*, vol. 5, no. 1, pp. 51–73, 2016.

[63] W. J. Fisk, D. Faulkner, J. Palonen, and O. Seppanen, "Performance and costs of particle air filtration technologies," *Indoor Air*, vol. 12, pp. 223–234, 2002.

[64] G. Liu *et al.*, "A review of air filtration technologies for sustainable and healthy building ventilation," *Sustain. Cities Soc.*, vol. 32, no. April, pp. 375–396, 2017.

[65] D. Lv, M. Zhu, Z. Jiang, S. Jiang, Q. Zhang, and R. Xiong, "Green electrospun nanofibers and their application in air filtration," *Macromol. Mater. Eng.*, vol. 1800336, no. 303, pp. 1–18, 2018.

[66] TSI, "Mechanisms of filtration for high efficiency fibrous filters," in *Application Note ITI-041*, 2012.

[67] A. Podgorski, A. Balazy, and L. Gradon, "Application of nanofibers to improve the filtration efficiency of the most penetrating aerosol particles in fibrous filters," *Chem. Eng. Sci.*, vol. 61, no. 20, pp. 6804–6815, 2006.

[68] J. Wang, S. C. Kim, and D. Y. H. Pui, “Investigation of the figure of merit for filters with a single nanofiber layer on a substrate,” *J. Aerosol Sci.*, vol. 39, pp. 323–334, 2008.

[69] Q. Zhang, J. Welch, H. Park, C.-Y. Wu, W. Sigmund, and J. C. M. Marijnissen, “Improvement in nanofiber filtration by multiple thin layers of nanofiber mats,” *J. Aerosol Sci.*, vol. 41, no. 2, pp. 230–236, 2010.

[70] R. Al-Attabi, L. Dumee, L. Kong, J. Schütz, and Y. Morsi, “High efficiency poly (acrylonitrile) electrospun nanofiber membranes for airborne nanomaterials filtration,” *Adv. Eng. Mater.*, vol. 1700572, no. 20, pp. 1–10, 2018.

[71] R. Al-Attabi, Y. Morsi, W. Kujawski, L. Kong, J. Schütz, and L. F. Dumée, “Wrinkled silica doped electrospun nano-fiber membranes with engineered roughness for advanced aerosol air filtration,” *Sep. Purif. Technol.*, vol. 215, no. December 2018, pp. 500–507, 2019.

[72] EN 1822, “High efficiency air filters (EPA, HEPA and ULPA).” 2009.

[73] W. H. Organization, “Guidelines for drinking-water quality, Chapter 7 (microbial aspects).” 2011.

[74] EPA, “Edition of the Drinking Water Standards and Health Advisories.” Office of Water, United States Environmental Protection Agency 822-S-12-001, 2012.

[75] M. Raza, Z. Kanwal, A. Rauf, A. Sabri, S. Riaz, and S. Naseem, “Size- and shape-dependent antibacterial studies of silver nanoparticles synthesized by wet chemical routes,” *Nanomaterials*, vol. 6, no. 4, p. 74, 2016.

[76] D. H. Kim, J. C. Park, G. E. Jeon, C. S. Kim, and J. H. Seo, “Effect of the size and shape of silver nanoparticles on bacterial growth and metabolism by monitoring optical density and fluorescence intensity,” *Biotechnol. Bioprocess Eng.*, vol. 22, no. 2, pp. 210–217, 2017.

[77] A. Chaudhary, A. Gupta, R. B. Mathur, and S. R. Dhakate, “Effective antimicrobial filter from electrospun polyacrylonitrile-silver composite nanofibers membrane for conducive environment,” *Adv. Mater. Lett.*, vol. 5, no. 10, pp. 562–568, 2014.

[78] D. Lv *et al.*, “Ecofriendly Electrospun Membranes Loaded with Visible-Light-Responding Nanoparticles for Multifunctional Usages: Highly Efficient Air Filtration, Dye Scavenging, and Bactericidal Activity,” *ACS Appl. Mater. Interfaces*, vol. 11, pp. 12880–12889, 2019.

[79] S. Pal, Y. K. Tak, and J. M. Song, “Does the Antibacterial Activity of Silver Nanoparticles Depend on the Shape of the Nanoparticle? A Study of the Gram-Negative Bacterium Escherichia coli,” *Appl. Environ. Microbiol.*, vol. 73, pp. 1712–1720, 2007.

Supporting Information

EFFICIENT NANOPARTICLES REMOVAL AND BACTERICIDAL ELECTROSPUN NANOFIBERS MEMBRANES FOR AIR FILTRATION

Ana Claudia Canalli Bortolassi[1], Sakthivel Nagarajan[2], Bruno de Araújo Lima[1], Vádila Giovana Guerra[1], Mônica Lopes Aguiar[1], Vincent Huon[3], Laurence Soussan[2], David Cornu[2], Philippe Miele[2] and Mikhael Bechelany[2]

[1]Universidade Federal de São Carlos – UFSCar, Departamento de Engenharia Química, Rodovia Washington Luiz, km 235 – SP 310, 13565-905 São Carlos, Brazil; tel. +55 16 3351 8269

[2]Institut Européen des Membranes, URM 5635, CNRS, ENSCM, Université Montpellier, Place Eugene Batailon, F-34095 Montpellier cedex 5, France.

[3]Laboratoire de Mécanique et Génie Civil, Université de Montpellier, CNRS, 34090Montpellier, France

E-mail: mikhael.bechelany@umontpellier.fr

The crystallinity of the silver nanoparticles was analyzed using X-ray diffraction analysis and shown in Figure S1. The peak observed at 17° for the 0AgF samples corresponds to (110) plan of PAN. Crystalline peak corresponds to silver nanoparticles were absent in all samples (1AgF, 10AgF, and 50AgF) which is due to the small size (<5nm) of silver nanoparticles.

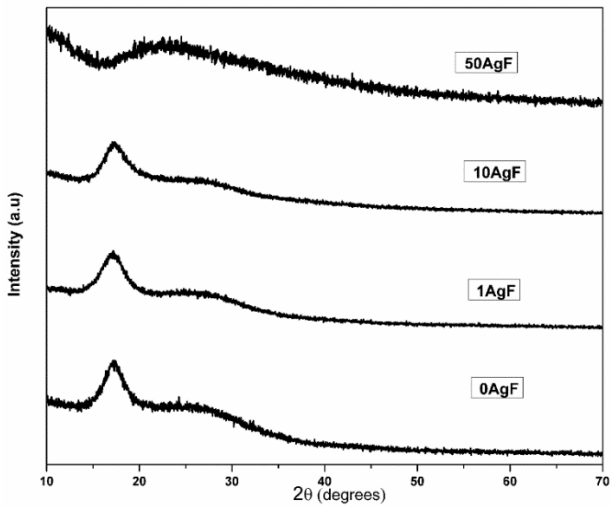

Figure S1 - XRD patterns of PAN and silver nanoparticles incorporated electrospun fibers

FTIR spectroscopy was used to identify the presence of functional groups on Ag/PAN nanofibers. Figure Figure S shows FTIR spectra of PAN nanofibers without and with silver nanoparticles in the range of 4000-700 cm^{-1}. No significant difference is observed when silver nanoparticles were introducing inside the nanofibers.

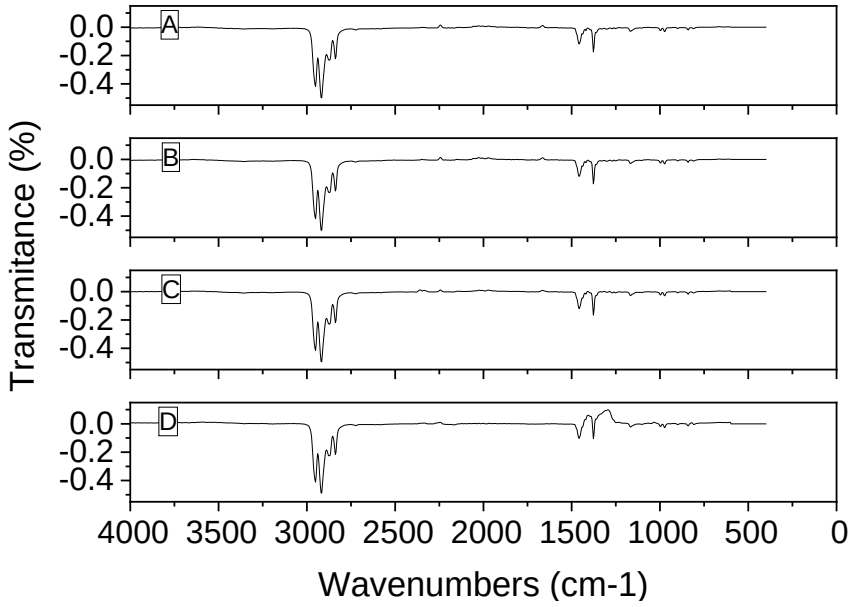

Figure S2 - FTIR spectra of Ag/PAN nanofibers (A)0AgF (B)1AgF (C)10AgF (D)50AgF

Energy dispersive X-ray spectroscopy based elemental mapping (EDX) were also performed to support the distribution of silver nanoparticles and are shown in Figure S3. EDX confirms that the silver is distributed uniformly throughout the PAN fibrous matrix.

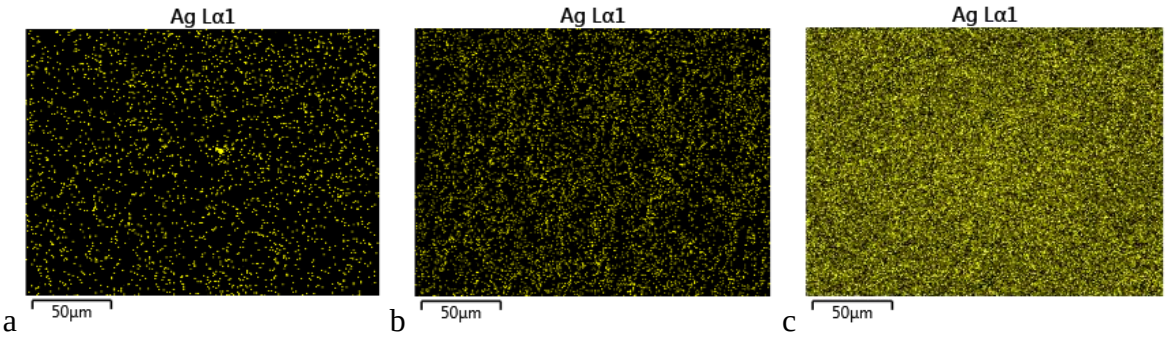

Figure S3- Elemental mapping images of Ag/PAN nanofibers a) 1AgF b) 10AgF c) 50AgF

Higher magnification TEM images of 0AgF and 50AgF were provided in the Figure S4. TEM image of 50AgF shows that the silver nanoparticles are distributed uniformly throughout the fibrous matrix. Histogram of silver nanoparticles size distribution were provided (inset image of 50AgF) and shows that the silver nanoparticles are below 5nm.

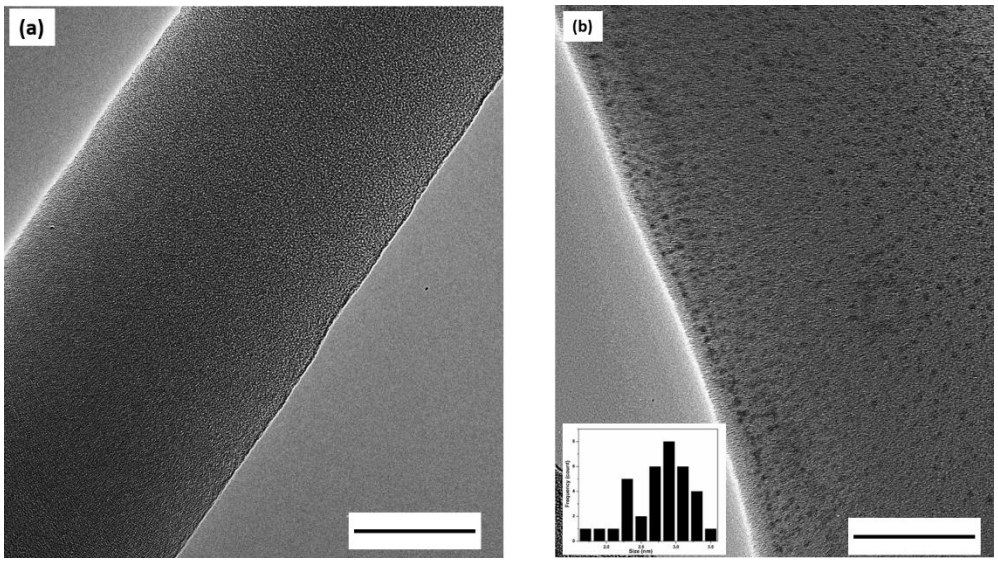

Figure S4. TEM images of (a) 0AgF, (b) 10AgF (scale bars are 50nm)

Table S1 Quantification of silver in electrospun fibers

Sample	Silver concentration in electrospun fibers (mg/g of PAN fibers)
0AgF	0
10AgF	57.4
50AgF	287.6